International Journal of Nanoelectronics and Materials
IJNeaM
ISSN 1985-5761 | E-ISSN 2232-1535

# Development of a Portable Gold Nanoparticle-Based Sensor for Rapid Malathion Detection

Nur Anis Aqilah Abdul Halim[a,b], Nur Liyana Razali[a,b], Marlia Morsin[a,b]*, Zarina Tukiran[c] and Suratun Nafisah[d]

[a] *Microelectronics & Nanotechnology – Shamsuddin Research Centre (MiNT-SRC), Institute for Integrated Engineering, Universiti Tun Hussein Onn Malaysia, 86400, Parit Raja, Batu Pahat, Johor, Malaysia*
[b] *Department of Electronics Engineering, Faculty of Electrical and Electronic Engineering, Universiti Tun Hussein Onn Malaysia, 86400, Parit Raja, Batu Pahat, Johor, Malaysia*
[c] *Internet of Things (IoT) Focus Group, Faculty of Electrical and Electronic Engineering, Batu Pahat, 86400, Universiti Tun Hussein Onn Malaysia.*
[d] *Department of Electrical Engineering, Institut Teknologi Sumatera (ITERA), Lampung Selatan, 35365, Indonesia*
*∗Corresponding author. Tel.: +0-000-000-0000; fax: +0-000-000-0000; e-mail: marlia@uthm.edu.my*

Received XXX 2023, Revised XXX 2023, Accepted XXX 2023

**ABSTRACT**

The widespread use of pesticides such as malathion in agriculture poses significant risks to human health, ecosystems, and food safety due to contamination of water, soil, and crops. Conventional methods for detecting pesticide residues are highly accurate but impractical for on-site monitoring due to their high cost, complexity, and time-consuming procedures. This study introduces a portable, cost-effective sensor system for real-time malathion detection, integrating gold nanobipyramids as sensing materials, a SparkFun Triad Spectroscopy Sensor, and an Arduino UNO microcontroller. The gold nanobipyramids, with a surface density of approximately 69.623% and an average aspect ratio of 1.65 ± 0.06, exhibit two resonance peaks: one around 556 nm, associated with transverse plasmon resonance (t-SPR), and another at 716 nm, corresponding to longitudinal plasmon resonance (l-SPR). Sensor responses were recorded through spectral shifts upon exposure to malathion. The spectroscopy sensor was calibrated to detect these shifts and integrated with the Arduino UNO for data processing and display. A custom 3D-printed casing made from biodegradable PLA material housed the system, ensuring portability and user-friendliness. Experimental results validated the sensor's capability to detect malathion with high precision, at concentrations as low as 0.5 mg/mL, offering a rapid and reliable alternative to conventional laboratory techniques. This portable device presents high potential for agricultural workers as an efficient tool for monitoring pesticide residues, supporting sustainable agricultural practices, reducing environmental pollution, and enhancing food safety.

**Keywords:** *Gold nanobipyramids, malathion detection, portable sensor, Arduino UNO, surface plasmon resonance (SPR) and agricultural monitoring*

## 1. INTRODUCTION

The presence of pesticide residues, particularly organophosphates such as malathion, has become a significant concern due to their adverse effects on both human health and the environment. Malathion is commonly used in agriculture but often lingers in the atmosphere, leading to the contamination of water and crops. This poses serious health risks to people, either through direct consumption or indirect exposure [1],[2]. Additionally, malathion can disrupt ecosystems by harming beneficial species, such as pollinators and soil microbes [3], which are essential for maintaining ecological balance and supporting sustainable farming practices.
Traditional methods for detecting pesticide residues, such as high-performance liquid chromatography (HPLC) and gas chromatography-mass spectrometry (GC-MS), are known for their accuracy [4]. However, these techniques often require expensive equipment, expert operators, and lengthy processes, making them impractical for immediate or on-site monitoring [5]. This limitation hampers timely efforts to address pesticide contamination in agriculture and the environment.
With the rise of nanotechnology, new possibilities have emerged for creating portable and rapid detection systems. Among various nanomaterials, gold nanobipyramids have shown great promise for sensing applications due to their unique optical, electrical, and chemical characteristics [6]. Their distinctive shape and increased surface area boost molecular interactions, leading to heightened sensitivity in detection [7].
One of the standout features of gold nanobipyramids is their surface plasmon resonance (SPR). This refers to a phenomenon where light causes electrons on the nanoparticle surface to resonate, generating unique optical signals. When specific substances like malathion come into contact with GNBPs, they cause detectable shifts in these SPR signals. This property allows for real-time monitoring of malathion levels with impressive sensitivity and specificity [8].
By combining gold nanobipyramids with spectroscopy sensors and microcontroller platforms, we can greatly enhance their effectiveness for portable detection systems. For example, the SparkFun Triad Spectroscopy sensor can detect changes in the spectrum resulting from interactions between nanoparticles and analytes over a broad range of

wavelengths [9]. This integration allows for accurate monitoring of malathion concentrations in real-time, providing a quick and practical solution for pesticide detection.

Using affordable microcontrollers like the Arduino UNO creates a user-friendly interface for processing the spectral data collected from these sensors. By utilizing Arduino, data from the SparkFun Triad Spectroscopy sensor can be analyzed to assess SPR shifts and display the malathion concentration in an easy-to-understand format. The practicality, portability, and cost-effectiveness of these systems make them excellent choices for real-time, on-site pesticide monitoring, giving users valuable insights into managing agricultural and environmental challenges [10].

In summary, combining gold nano bipyramids, spectroscopy sensors, and microcontroller platforms offers an innovative approach to creating compact, efficient, and affordable systems for detect malathion residues. These advancements are vital in enhancing food safety, decreasing environmental pollution, and supporting sustainable agricultural practices.

In this research, the fabrication of gold nanoparticles with a bipyramid shape is performed to serve as a sensing material. This sensing material was used in a portable sensor system. This sensor system was developed using the SparkFun Triad Spectroscopy sensor integrated with an Arduino UNO microcontroller, an LED, and the synthesized gold nanoparticles for the detection of malathion.

## 2. MATERIALS AND METHODS

This study consists of four stages: 1) Fabrication and characterization of gold nanobipyramids as sensing materials, 2) Preparation of malathion solution and Sensor Testing, 3) Casing design of the Portable Sensor, and 4) Implementation of Hardware in the Sensor System. Each of the stages was explained in the next section.

### 2.1 Fabrication and Characterization of Gold Nanobipyramids as Sensing Material

The synthesis of gold nanobipyramids was carried out using the Seed Mediated Growth Method (SMGM) following the recipe established in our previous work [11],[12]. The materials used for this work are gold (III) chloride trihydrate ($HAuCl_4.3H_2O$), chloroplatinic acid hydrate ($H_2PtCl_4.H_2O$), hexacetyltrimethylammonium bromide ($C_{19}H_{42}Br$), sodium borohydride ($NaBH_4$), ascorbic acid ($C_6H_8O_6$) purchased from Sigma Aldrich (USA). Then, hydrochloric acid (HCl) and silver nitrate ($AgNO_3$) are purchased from RCI Labscan (Thailand). All the materials are diluted in deionized water (DIW) with a resistivity of 18.2 MΩcm.

For the characterization, the synthesized gold nanobipyramids were tested using UV-1800 Shimadzu Spectrophotometer, Japan, with a wavelength range of 400 – 1 000 nm for optical properties, a Bruker D8 Advance X-Ray Diffractometer, Germany, with the range of 20º - 60º for structural properties, and the FESEM Joel JSM-7600, USA, with a magnification of 100 000X for morphological properties.

### 2.2. Preparation of Malathion Solution and Sensor Testing

The target analyte, malathion, used in this study is in the form of a commercialized pesticide produced by MAPA, registered under the number LRMP.R/6314. This Malathion has a concentration of 57%. In order to study the effect of concentration, the Malathion stock solution with 57% concentration was diluted to vary the Malathion solution concentration from 0.05% to 0.9% (0.5 – 9.0 mg/mL). Each Malathion concentration was prepared in a volume of 20 mL of solution.

As previously explained, gold nanobipyramids were used as a sensing material for malathion detection. There are three tests performed in this study, namely the sensitivity test, selectivity test, stability test, and repeatability test. Each test was repeated no less than four times to ensure precise results. The details of each test are explained as follows:

**(a) Sensitivity test**

This test evaluates the detection limits of the gold nanoparticle-based sensors for identifying pesticide residues. The sensitivity test focuses on assessing the response of the sensor to various combinations of nanobipyramids and malathion. The results help determine the effectiveness and detection range of the system. The four samples used are 3.0 ml of 1) pure malathion, 2) pure gold nanobipyramids, 3) a mixture of Malathion and gold nanobipyramids, and finally 3.0 ml of DI water as a baseline.

Then, the sensitivity tests towards 10 different concentrations of malathion, starting from 0.5ml with an interval of 0.5 mL, were performed with a base of 2.5 mL of gold nanobipyramids.

**(b) Repeatability test**

A repeatability test was conducted by sequentially recording an absorption spectrum in two different media. This test was performed over five cycles. In this study, the assessment of repeatability involved alternating between medium 2.5 mL of gold nanobipyramids combined with 0.5 mL of Malathion for the first medium and 0.5 mL of DI water for the second medium. This step involves multiple iterations to ensure that the sensor provides consistent readings under identical conditions.

**(c) Stability test**

Stability testing examines the durability and operational lifespan of the sensors. The sample of 3.0 mL mixture of gold nanobipyramids and 0.5 mL of malathion. was running for 600 seconds.

### 2.3. Casing Design of the Portable Sensor

The casing of the portable sensor was designed in SketchUp software, as shown in Figure 1(a-c). For the prototyping phase, polylactic acid (PLA) was selected as the material due to its lightweight properties, which contribute to the overall portability of the device. Additionally, the PLA's biodegradable nature supports environmentally sustainable design practices, aligning with current trends in green engineering.

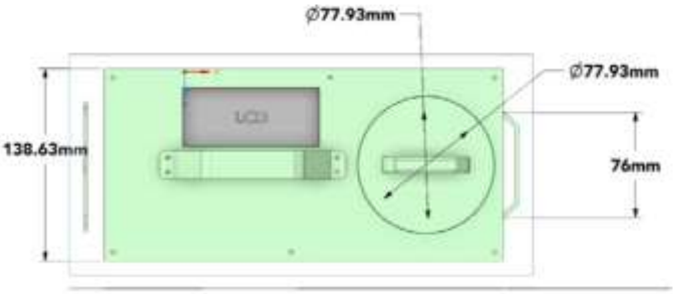


**(a)** Top view

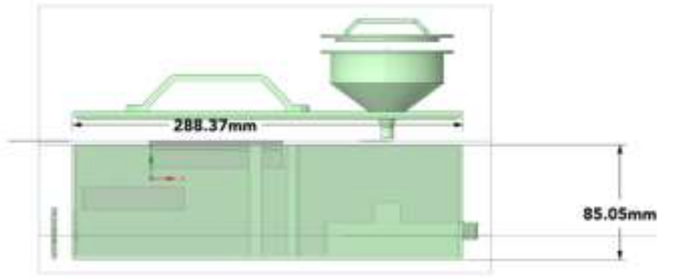


**(b)** Side view

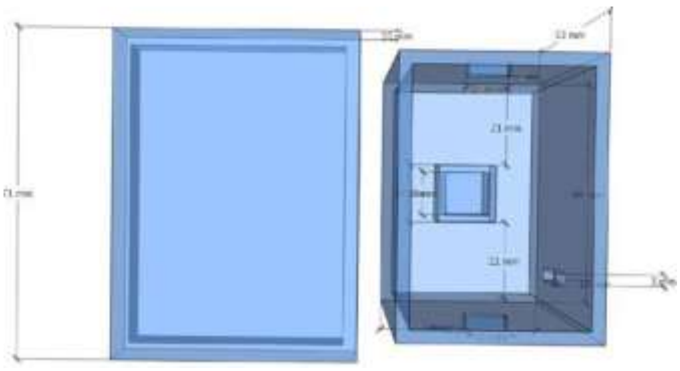

**(c)** Inside view

**Figure 1**. Design of the portable casing

## 2.4. Implementation of Hardware in Sensor Setup

The developed portable sensor comprises two distinct hardware modules: the sensing module and the microcontroller unit (MCU) module. The sensing module is responsible for detecting the presence of Malathion in the sample, while the MCU module functions as both the controller and communication interface for the sensing operations. The system is powered externally by a 4000 mAH power bank, enabling portable and uninterrupted operation.

For user interaction, a 20x4 Inter-Integrated Circuit (I2C) liquid crystal display (LCD) module is integrated into the device to display real-time measurement results. In addition to presenting output data, the LCD also provides status updates, notifying the user of successful operations or any errors encountered during testing. A comprehensive view of the implemented hardware components and their configuration is presented in Figure 2.

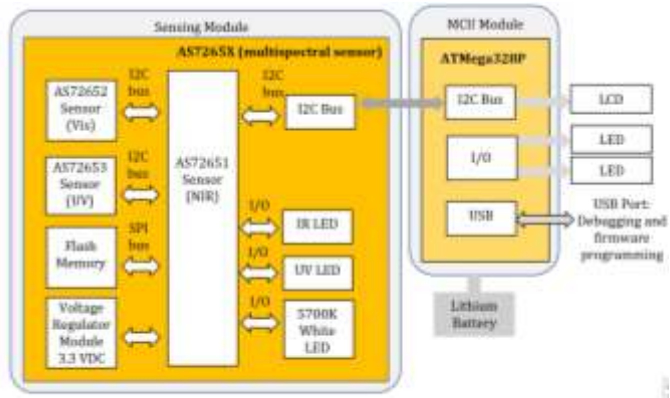


**Figure 2**. Implemented hardware on the AS7265X-based sensing module and the MCU module

### 2.4.1. Sensing Module

The sensing module comprises the gold nanoparticle-based sensor and the AS7265X multispectral sensor, integrated with the MCU via the I2C bus. The gold nanoparticle-based sensor is housed in a standard optical cuvette with dimensions of 1.1 cm x 1.1 cm x 4.4 cm, as illustrated in Figure 3.

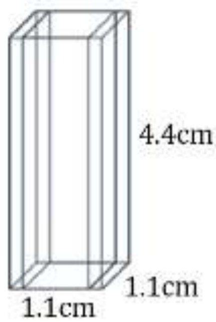


**Figure 3**. The optical cuvette holds the gold nanoparticles-based sensor

The AS7265X sensor from Sparkfun is a composite of three individual sensors: AS72651, AS72562 and AS72653 - collectively offering 18 discrete spectral channels, as shown in Figure 4 [13]. These sensors cover three spectral ranges: the AS72651 for near-infrared (NIR) wavelengths (610-860 nm), the AS72652 for visible light (Vis) wavelengths (560-940 nm), and the AS72653 for ultraviolet (UV) wavelengths (410-535 nm). The AS7265X sensor also features a programmable light-emitting diode (LED) electronic shutter and includes three (3) embedded LEDs: 5700 Kelvin White LED, 402 nm Ultraviolet LED, and 875 nm Infrared LED, which serve as external illumination sources for the sample during measurement.

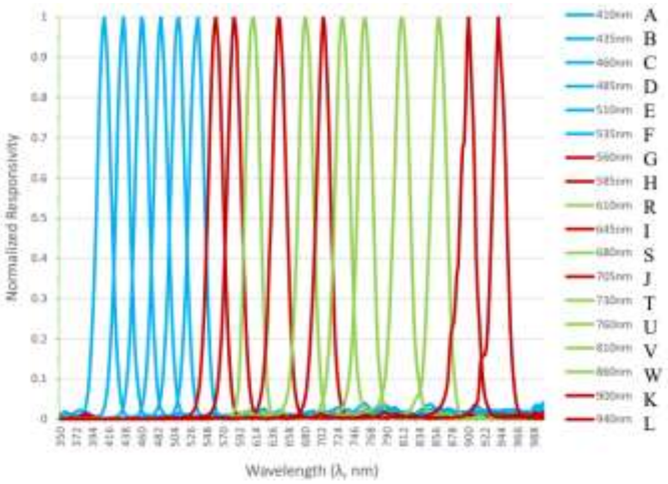


**Figure 4**. The 18 wavelengths supported by the AS7265X sensor

### 2.4.2. MCU Module

The MCU module is built around an 8-bit ATmega328P from Arduino [14]. In this work, the MCU was programmed to acquire spectral measurements from the sensing module in order to detect the presence of Malathion. The results were then processed and displayed in real-time via the integrated LCD module.

## 3. RESULTS AND DISCUSSION

### 3.1 Results of Fabrication and Characterization of Gold Nanobipyramids

In this first stage of the project, gold nanobipyramids were successfully synthesized using the Seed-Mediated Growth Method (SMGM). The characterization of these nanoparticles confirmed their desired shape and properties. The UV-Vis spectroscopy revealed distinct surface plasmon resonance (SPR) peaks, indicating the successful formation of gold nanoparticles with enhanced optical properties. The X-ray Diffraction analysis confirmed the crystalline nature of gold nanoparticles. The FESEM images showed that the nanoparticles were uniform in size and shape, with clear bipyramidal morphology.

The absorption spectrum in the UV-Vis range for the synthesized gold nano bipyramids is shown in Figure 5, highlighting two prominent localized surface plasmon resonance (LSPR) peaks that offer valuable information regarding the optical characteristics of the material. The first peak, found around 556 nm, is associated with the transverse plasmon resonance (t-SPR), signifying the oscillation of electrons along the shorter axis of the nano bipyramids. In contrast, the second peak, which occurs at a longer wavelength of 716 nm, corresponds to the longitudinal plasmon resonance (l-SPR), linked to electron oscillation along the longer axis of the bipyramids.
The observation of these two peaks not only validates the anisotropic characteristics of the gold nanobipyramids but also demonstrates the distinctive interactions between conduction electrons and light that arise from the nanoparticles' geometry. Additionally, a shoulder peak is noted around 513 nm in the spectrum, which is attributed to electron oscillations in by-products that exhibit nanosphericals shape. This shoulder peak adds further insight into the formation of secondary nanoparticles during the synthesis.

The calculated intensity ratio of the normalized l-SPR to t-SPR bands stands at 2.1:1. This notable intensity ratio indicates a relatively high yield of anisotropic nanoparticles and suggests that the sample predominantly contains well-formed bipyramids. An increased intensity of the l-SPR is directly associated with the presence of well-defined nano bipyramids, as it signifies their capacity to sustain stronger plasmonic excitations.

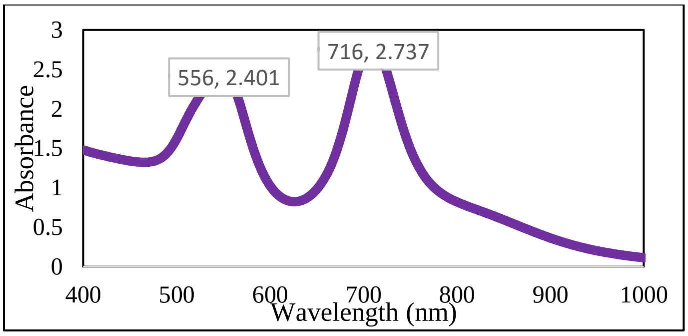


**Figure 5.** UV-Vis absorbance spectrum of gold nanobipyramids

An X-ray diffraction (XRD) analysis was conducted to assess the crystallinity and structural features of the GNBPs. The XRD pattern displayed in Figure 6 shows two prominent peaks at 38.17° and 51.07°, which correspond to the (111) and (200) crystallographic planes of gold (Au), respectively. These planes are typical of the face-centered cubic (FCC) crystalline structure, confirming the creation of crystalline gold nanostructures.
The calculated lattice constant for the FCC Au structure was found to be 4.08 Å, aligning with the standard value for gold and further supporting the crystalline character of the synthesized GNBPs. Furthermore, the crystallite sizes for the (111) and (200) planes were 202.4548 Å and 321.9135 Å, respectively. These findings imply that the GNBPs demonstrate high crystallinity and structural uniformity. The sharp and narrow XRD peaks suggest that the produced GNBPs possess well-defined and consistent structural characteristics, which are essential for their potential applications.

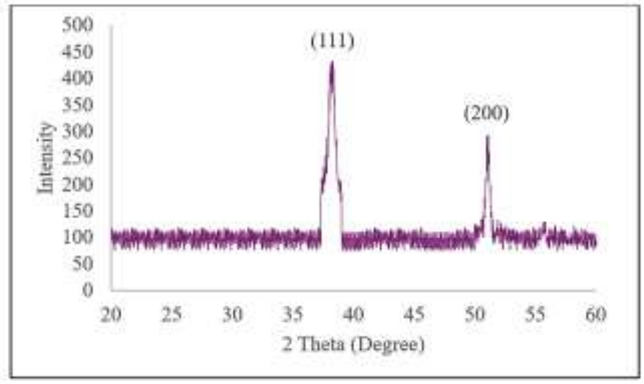


**Figure 6**. The XRD pattern of gold nanobipyramids

The FESEM image in Figure 7 provides a comprehensive view of the successful synthesis of gold nano bipyramids (GNBPs), illustrating a substantial yield of these nanostructures. The bipyramid morphology, characterized by two pyramids that share a common base, is distinctly highlighted in the micrograph, which captures the intricate features of the gold nanobipyramids. The quantitative analysis of the image reveals that the particles exhibit a highly uniform size distribution with surface density ~ 69.623 %. The average length of these nanoparticles is determined to be 56.46 ± 0.81 nm, while the average width measures 36.36 ± 1.83 nm, resulting in an average aspect ratio of 1.65 ± 0.06. This consistent dimensionality suggests that the growth process was rigorously controlled, culminating in nanoparticles of exceptional homogeneity.

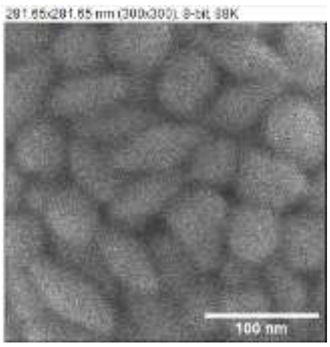


**Figure 7.** FESEM image of GNBPs of three different areas

## 3.2. Results of Sensor Testing

### (a) Sensitivity Test

The sensitivity test focuses on evaluating the sensor's response to various combinations of gold nanobipyramids and malathion. The results revealed distinct shifts in LSPR peaks for the samples tested, which correlate strongly with the refractive index values. Notably, the sample comprising nanobipyramids and 6.0 mg/mL with refractive index of 1.00103) exhibited the largest LSPR peak shift of 654 nm, highlighting the significant impact of malathion concentration on the local dielectric environment.

In comparison, pure malathion displayed a peak shift of 546 nm, attributed to the higher refractive index of the concentrated solution. Pure gold nanobipyramids generated a peak shift of 419 nm, reflecting their inherent sensitivity to variations in the surrounding medium. Deionized water, with the lowest refractive index, resulted in the minimal peak shift of 81 nm, underscoring the sensor's capability to differentiate between highly contrasting refractive index environments. Figure 8 shows the sensitivity test of the sensor.

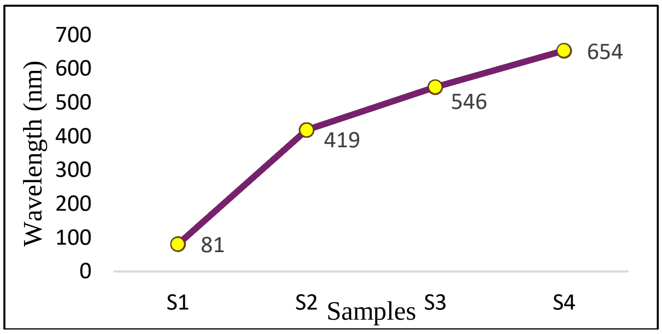


**Figure 8.** Result for sensitivity test S1) pure malathion, 2) pure gold nanobipyramids, S3) a mixture of Malathion and gold nanobipyramids, and S4) 3.0 ml of DI water as a baseline.

The linear relationship between malathion concentration and refractive index is similar to the theory, indicating a reliable performance. As malathion concentration increases, the refractive index also rises proportionally, leading to more pronounced LSPR peak shifts. This trend emphasizes the gold nanobipyramids-based sensor's effectiveness in detecting malathion levels across a wide concentration range, from as low as Sample 1 (0.5 mg/mL, η = 1.000086) to as high as Sample 10 (9.0 mg/mL, η = 1.00155). Figure 9 shows the sensitivity results towards variation concentration of malathion.

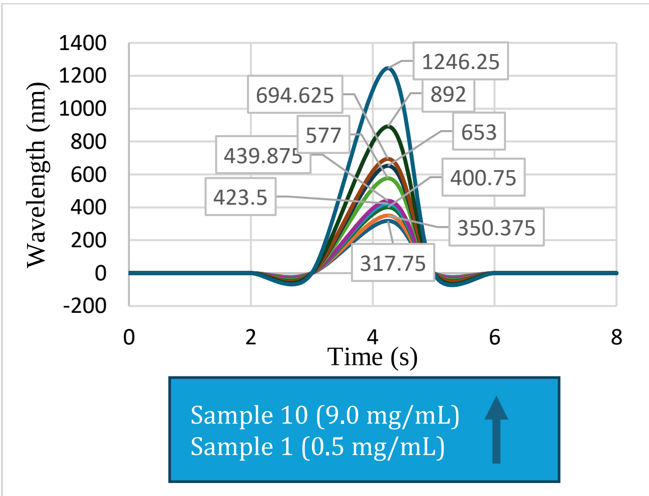


**Figure 9.** Result for sensitivity towards different concentration of malathion.

The results affirm the sensor's robustness and reliability, making it ideal for practical applications in agricultural monitoring and quality control. Its ability to detect malathion levels below the maximum residue limit (MRL) of 8 mg/mL ensures its feasibility for maintaining food safety in products like pineapples.

### (b) Repeatability Testing

Two samples were prepared: Sample R1 with gold nanoparticles mixed with malathion solution and SampleR2 with GNBPs and deionized (DI) water as a control. The refractive index of the malathion solution was compared to that of DI water, which is 1.3330. Each sample underwent five testing cycles to assess the sensor's performance. For Sample R1, the LSPR peak values ranged from 260 nm to 268 nm consistently, indicating the sensor's sensitivity to changes in the malathion solution's refractive index. In contrast, Sample R2 showed minimal shifts, confirming the lack of response to DI water. The repeatability result is shown in Figure 10.

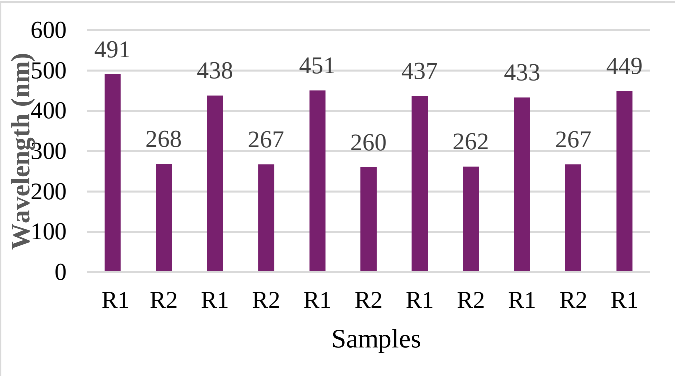


**Figure 10.** The Repeatability Result of the sensor

The maximum deviation of peak shifts for Sample R1 was within ±1 nm, highlighting the sensor's repeatability and precision. These results affirm the sensor's reliability for detecting chemical variations, paving the way for future applications in environmental monitoring and safety assessments. Overall, the study reinforces the importance of repeatable measurements in advancing sensor technology for effective chemical detection.

### (c) Stability Testing

In this analysis, a stability test was performed to observe the behavior of a sensor utilizing Localized Surface Plasmon Resonance (LSPR) while interacting with a malathion solution (M2) at a concentration of 1.0 mg/mL. The foundation of the stability test revolved around precise sample preparation, which involved mixing 2.5 mL of gold nanoparticles with 0.5 mL of malathion solution. In order to ensure accurate analysis, the sensor response was observed over a defined duration of 600 seconds (10 minutes). During this period, the LSPR peak shift was continuously monitored to identify any variations that might suggest instability in the sensor's performance when exposed to a constant refractive index.

Throughout the testing duration, the LSPR peak was recorded at regular intervals as shown in Figure 11. The primary focus was to detect any fluctuations in the peak shift, a vital indicator of the sensor's stability. The results were promising; the LSPR peak values maintained consistent readings at 261 nm for most of the test period. While minor fluctuations of ±1 nm were recorded, these variations fell well within the acceptable range, thereby affirming the sensor's reliability. Additionally, the minimal variation observed in the sensor's response highlighted its robustness under prolonged exposure to the malathion solution. The overall consistency in reading reinforced the idea that the sensor is effective in maintaining stability despite environmental influences.

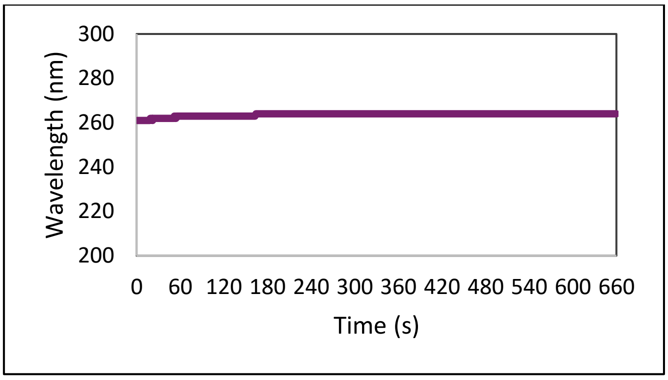


**Figure 11.** The Stability Result of the sensor

### 3.3. Results of Casing Design for the Portable Sensor

The prototype of the portable sensor, depicted in Figures 12 and 13, was fabricated using PLA material. Figure 12 (left) presents the top view of the assembled prototype, while Figure 12 (right) shows the internal view of the sensing module with its cover removed. Figure 9 shows the internal configuration of the sensor, highlighting the arrangement of both the sensing and the MCU modules. The prototype features a matte black surface finish, which was intentionally selected to minimize stray light interference and thereby improve the accuracy of spectral measurement.


**Figure 12**. The top view of the portable sensor when the sensing module is covered (left) and removed (right)

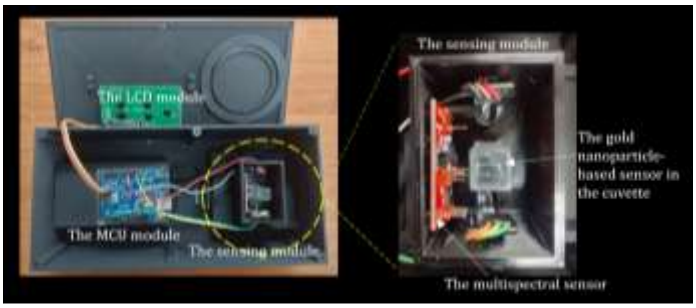


**Figure 13**. The inside view of the portable sensor; the arrangement of the sensing and MCU modules (left) and the close-up of the inside view of the sensing module (right)

### 3.4. Results of The Implemented Hardware

As previously described, the portable sensor system comprises two main modules: the sensing module and the MCU module. Prior to the full system integration, functional testing was performed on key components: the AS7265X multispectral sensor and the LCD, to ensure they were free of defects and operating as intended. During these tests, each component was individually connected to the MCU module ATmega328P to execute designated tasks. The performance and output of each component were monitored using the integrated development environment (IDE), specifically via the serial monitor and serial plotter tools.

For the AS7265X multispectral sensor, functional testing involved establishing a direct connection between the sensor and the MCU module, followed by programming the MCU to execute light calibration routines. The calibration results were visualised on the IDE via the serial plotter tool as shown in Figure 14. The appearance of distinct spectral peaks confirmed successful sensor calibration under light exposure, indicating proper sensor functionality.

**Figure 14**. Light calibration of the multispectral sensor on the plotter

Figure 15 presents the results of the LCD functional testing, as observed on the serial monitor. In this test, the LCD was interfaced with the MCU module, and the MCU was programmed to display predefined text messages following successful system initialization. This process verified that the LCD was functioning correctly and capable of displaying output as expected.


**Figure 15**. The result of the LCD on the serial monitor

Figure 16 shows the final implementation of the portable sensor hardware. As shown in Figure 12 (top left), the operational status of the sensor is communicated to the user via the LCD display. Meanwhile, Figure 16 (top right) depicts the external LEDs within the sensing module illuminating the sample during the detection process. The presence of Malathion was identified by the multispectral sensor through the observation of the spectral shifts, which are indicative of interactions between gold nanoparticles and Malathion molecules.

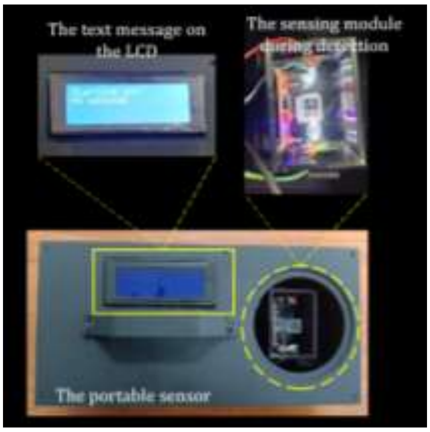


**Figure 16**. The result of the implemented hardware of the portable sensor

## 4. CONCLUSION

The study shows the potential of gold nanoparticles, particularly those with a bipyramidal shape, as effective sensing materials for pesticide detection. The enhanced surface plasmon resonance properties of these nanoparticles significantly contributed to the sensor's sensitivity, allowing it to detect malathion at low concentrations. The integration of the SparkFun Triad Spectroscopy Sensor with the Arduino UNO microcontroller proved to be an efficient and cost-effective solution for real-time detection and data processing. The compact design and integration of a biodegradable PLA casing make the device ideal for on-site detection of malathion, providing farmers and environmental specialists with a rapid and accessible tool for monitoring pesticide contamination. Furthermore, the sensor's ability to detect malathion in real-time offers a significant advantage over traditional laboratory-based techniques, which often require extensive time and resources.

However, there are some limitations to consider. While the sensor demonstrated excellent performance in detecting malathion, it may require further optimization to improve its detection range for even lower concentrations or other pesticide residues. Additionally, the real-world application of the sensor in diverse environmental conditions needs to be further evaluated to ensure its robustness and reliability under different field circumstances.

In conclusion, the results from this project highlight the effectiveness of using gold nanoparticle-based sensors for detecting pesticide residues like malathion. The system's portability, sensitivity, and real-time detection capabilities offer a promising solution for agricultural monitoring, contributing to safer farming practices and environmental sustainability. Future improvements could focus on enhancing the sensor's performance in detecting a broader range of pesticides and ensuring its adaptability for various field conditions.

**CONFLICT OF INTEREST**

Marlia Morsin and Zarina Tukiran are currently serving as academicians at Universiti Tun Hussien Onn Malaysia. Nur Anis Aqilah and Nur Liyana Razali are research students under the supervision of Marlia Morsin. Suratun Nafisah is a lecturer at Insitut Teknologi Sumatera (ITERA).

**FUNDING**

This research work was supported financially by Research Management Centre (RMC), Universiti Tun Hussein Onn Malaysia, through the Tier 1 Grant (Q893). The authors thank Microelectronics & Nanotechnology-Shamsuddin Research Centre (MiNT-SRC), Universiti Tun Hussein Onn Malaysia, for the related facilities.

**ETHICAL APPROVAL**

This work is original and has not been published and submitted simultaneously for publication elsewhere.

**REFERENCES**

[1] World Health Organization. (2023). *Pesticides and their impact on health*. Retrieved from [World Health Organization].

[2] Singh, B., & Singh, K. (2021). Environmental persistence of pesticides and its impact on ecological health. *Journal of Environmental Research, 45*(2), 123–137.

[3] Qureshi, M., et al. (2020). Role of pesticides in disrupting soil ecosystems. *Agricultural Ecosystems & Environment, 187*, 82–91.

[4] Chen, X., et al. (2019). Advances in analytical techniques for pesticide residue detection. *Analytical Chemistry Review, 12*(3), 150–175.

[5] Li, P., et al. (2022). Challenges and solutions for on-site pesticide detection. *Environmental Monitoring Systems, 8*(1), 45–60.

[6] Elahi, N., et al. (2018). Gold nanoparticles in molecular sensing: A review. *Biosensors and Bioelectronics, 22*(5), 570–589.

[7] Zhang, J., et al. (2021). Surface plasmon resonance of gold nanobipyramids in environmental sensing. *Nano Research, 14*(7), 1248–1260.

[8] Kumar, A., & Gupta, P. (2023). SPR-based detection techniques for pesticides. *Journal of Nanotechnology Applications, 16*(4), 321–334.

[9] SparkFun Electronics. (n.d.). Triad Spectroscopy Sensor User Guide. Retrieved from [https://www.sparkfun.com/].

[10] Arduino Team. (2022). Using Arduino for environmental sensing. Retrieved from [https://www.arduino.cc/].

[11] Nafisah, S., Morsin, M., Sanudin, R., Razali, N. L., Zain, Z. M., & Djamal, M. (2022). Gold nanobipyramids as LPSR sensing materials for glyphosate detection: Surface density and aspect ratio effect. *IEEE Sensors Journal*, *22*(19), 18479-18485.

[12] Nafisah, S., Morsin, M., Iwantono, I., Sanudin, R., Zain, Z. M., Satria, L., ... & Mardiansyah, D. (2023). Growth time dependency on the formation of gold nanobipyramids for efficient detection towards chlorpyrifos-based LSPR sensor. *Optik*, *289*, 171270.

[13] https://look.ams-osram.com/m/76ce4c0d80cd1565/original/AS7265x-DS000612.pdf

[14] https://components101.com/microcontrollers/arduino-uno